https://doi.org/10.5194/esurf-2022-4
Preprint. Discussion started: 20 January 2022

Earth Surface Dynamics Discussions

Stochastic description of the bedload sediment flux

J. Kevin Pierce[1], Marwan A. Hassan[1], and Rui M.L. Ferreira[2]

[1]The University of British Columbia, Vancouver, Canada
[2]Instituto Superior Técnico, Lisbon, Portugal

Correspondence: K. Pierce (kevpierc@mail.ubc.ca)

Abstract. We present a new formulation of the bedload sediment flux probability distribution. Individual particles obey Langevin equations which are switched on and off by particle entrainment and deposition. The flux is calculated as the rate of many such particles crossing a control surface within a specified observation time. Flux distributions inherit observation-time dependence from the on-off motions of particles. At the longest observation times, distributions converge to sharp peaks around classically-expected values, but at short times, fluctuations are erratic. We relate this scale dependence of bedload transport rates to the movement characteristics of individual grains. This work provides a statistical mechanics description for the fluctuations and observation-scale dependence of sediment transport rates.

1 Introduction

Bedload transport refers to conditions when grains bounce and skid along the riverbed (Church, 2006). Numerous applications require predictions of bedload transport rates: ecological restoration, river engineering, and landscape evolution modeling provide examples. Predicting bedload fluxes is notoriously difficult, in part because they display wide fluctuations (Bunte and Abt, 2005; Recking et al., 2012). Considering this, any prediction of the bedload flux should really be supplemented by estimates of variability and the space or time scales over which averaged values converge.

Particle-based, stochastic approaches have been developed from which mean values, probability distributions, and averaging scales can all be obtained (e.g. Ancey and Pascal, 2020; Turowski, 2010). These approaches provide a more complete description of bedload transport than classic descriptions (e.g. Kalinske, 1947; Bagnold, 1966). However they remain largely kinematic in comparison, because they do explicitly incorporate the grain-scale mechanics (Furbish et al., 2021). In this paper, we provide a stochastic formulation of the bedload flux based directly on grain-scale mechanics. To achieve this, we first develop an improved Newtonian model of particle displacement which is applicable across a broad range of timescales.

The original description of bedload displacement is due to Einstein, who calculated bedload displacement as a random sequence of rests interrupted by instantaneous steps (Einstein, 1937). Later, Lisle et al. (1998) and Lajeunesse et al. (2017) improved Einstein's approach by promoting his instantaneous steps to intervals of motion with constant velocity. Their approach can be summarized with the stochastic equation

$$\dot{x}(t) = V\sigma(t), \tag{1}$$

https://doi.org/10.5194/esurf-2022-4
Preprint. Discussion started: 20 January 2022

where $x(t)$ is the sediment position, V is the constant velocity of moving grains, and $\sigma(t)$ is a dichotomous noise which flips randomly between $\sigma = 0$ (rest) and $\sigma = 1$ (motion) (e.g. Bena, 2006). Owing to the constant velocity assumption, this model for sediment displacement applies only at long timescales when the details of individual particle movements become irrelevant (cf. Weiss, 1994). To calculate displacements at short timescales, we should replace V with a mechanistic velocity derived from the forces on moving particles.

The velocities of moving grains fluctuate due to turbulent forcing and particle-bed collisions (Heyman et al., 2016; Fathel et al., 2015). Experiments indicate that downstream velocity distributions of particles can be exponential (Fathel et al., 2015; Lajeunesse et al., 2010), Gaussian (Heyman et al., 2016; Ancey and Heyman, 2014), or Gamma-like (Liu et al., 2019; Houssais et al., 2015). Several studies have successfully modeled the velocity fluctuations of moving particles by analogy to Brownian motion (Fan et al., 2014; Ancey and Heyman, 2014). These studies represent exponential and Gaussian velocities with the Langevin equation

$$\dot{v}(t) = F(v) + \xi(t), \tag{2}$$

where $v(t)$ is the sediment velocity, $\xi(t)$ is a random force, and $F(v)$ is a deterministic force. $\xi(t)$ is modeled as a Gaussian white noise for simplicity, although in principle this is not required. The choice $F(v) = -\mu v/|v| + \Delta$ produces exponential velocities, with μ a Coulomb friction coefficient and Δ a steady force per unit mass, while $F(v) = \gamma(V - v)$ produces Gaussian velocities, with γ an inverse relaxation time and V a steady-state velocity. Eq. (2) provides a reasonable description of bedload velocities over short timescales, but it cannot describe particle displacements over longer timescales, when entrainment and deposition also moderate transport.

Motion-rest alternation and the fluctuating movement velocities of individual particles both lend variability to the sediment flux (Böhm et al., 2004; Roseberry et al., 2012). Sediment fluxes have been defined with both surface and volume definitions (Ballio et al., 2014, 2018). The *ensemble averaged* sediment flux across a surface was formulated by Furbish et al. (2012, 2017):

$$\langle q(x,t)\rangle = \int_0^\infty dx' \int_0^\infty dt' R(x',t') E(x-x',t-t'). \tag{3}$$

This “nonlocal formulation" generalizes earlier approaches based on aggregating particles from upstream locations (Nakagawa and Tsujimoto, 1976; Parker et al., 2000). $E(x-x',t-t')$ is the entrainment rate a distance x' upstream a time t' in the past, while $R(x',t')$ is the probability that a just-entrained particle displaces *at least* a distance x' in time t'. For the steady case $E(x,t) = E$ where particles step an average distance ℓ in a motion, the nonlocal flux becomes $\langle q\rangle = E\ell$ in accord with Einstein (1950). The nonlocal formulation has not been extended to describe sediment transport fluctuations.

Both renewal theory and population modeling approaches describe a *stochastic* sediment flux by introducing additional Eulerian characteristics of particle transport. Renewal approaches introduce inter-arrival time distributions $\psi(t)$, characterizing intervals between successive arrivals of particles to a surface (Turowski, 2010; Ancey and Pascal, 2020). The flux is phrased as the rate of particle crossings over an observation time T:

$$q(T) = \frac{\mathcal{N}(T)}{T}. \tag{4}$$

https://doi.org/10.5194/esurf-2022-4
Preprint. Discussion started: 20 January 2022

$\mathcal{N}(T)$ is the number of particle crossings by T – related to $\psi(t)$. For exponential inter-arrival times $\psi(t) = \lambda e^{-\lambda t}$, the flux becomes Poissonian with *rate constant* λ, and its mean value is $\langle q \rangle = \lambda$. For other $\psi(t)$'s, the mean flux depends on the observation time T (scale dependence). Population approaches introduce Eulerian entrainment and deposition rates to count the number of moving particles in a volume (Ancey et al., 2006, 2008). Fluxes are then computed by summing the velocities of all moving particles in the volume. Both approaches provide excellent correspondence with experimental data. However, we still have little understanding of how to relate their Eulerian input parameters to grain-scale mechanics (cf. Heyman et al., 2016).

In this paper, our objective is to formulate the stochastic sediment flux directly from the dynamics of individual grains, rather than by introducing additional Eulerian quantities such as volumetric entrainment and deposition rates or inter-arrival time distributions. To achieve this, in Sec. 2 we extend the motion-rest alternation model for particle displacement, Eq. (1) to include Newtonian velocities from Eq. (2). This produces a description of particle displacement which is valid across timescales. We then construct the sediment flux in Sec. 3 by aggregating over individual particle displacements from this model. The resulting formulation shares elements from both the nonlocal and renewal approaches summarized in Eqs. (3) and (4). In Sec. 4 we solve the formulation for to derive the displacement and sediment flux probability distribution functions of bedload particles, and in Secs. 5 and 6 we discuss the new features and limitations of our approach, summarize its relationship to earlier work, and suggest several directions for further development.

2 Stochastic description of bedload transport

The starting point for our analysis is an idealized one-dimensional domain populated with sediment particles on the surface of a sedimentary bed. Particles are set in motion by the turbulent flow and move downstream until they deposit, and the cycle repeats. The downstream coordinate is x, so that $\dot{x} = v$ describes a velocity in the downstream direction and $\dot{v}$ describes an acceleration. The flow is considered weak enough that interactions among moving grains are uncommon, although interactions between moving particles and the bed occur regularly. These conditions are characteristic of rarefied bedload transport conditions (e.g. Kumaran, 2006; Furbish et al., 2017). Particles are considered to have similar enough shapes and sizes so as to have nearly identical mobility characteristics. These conditions allow for all particles to be described as independent from one another but governed by the same underlying dynamical equations. Any of these conditions could be relaxed in exchange for additional mathematical difficulty.

2.1 Mechanistic formulation of intermittent transport

From these assumptions, we propose an equation of motion for the individual sediment grain including two features. First, particles should alternate between motion and rest, similar to the earlier motion-rest models summarized by Eq. (1). Second, the velocities of moving particles should evolve according to the Newtonian equation (2). These dynamics can be represented

https://doi.org/10.5194/esurf-2022-4
Preprint. Discussion started: 20 January 2022

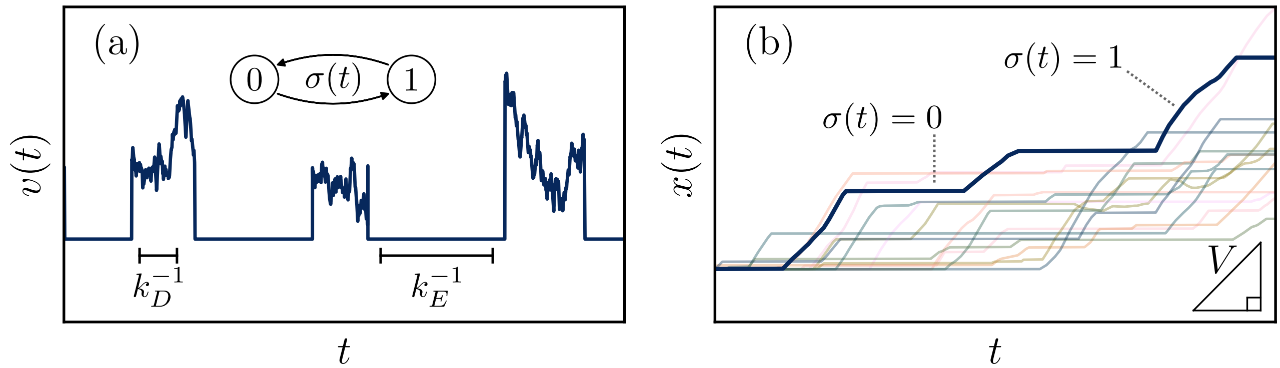

Figure 1. Panel (a) shows the velocity from Eq. (5) for a particular realization of the noises $\xi(t)$ and $\sigma(t)$, while panel (b) shows the position derived Eq. (5) alongside other possible trajectories. Keys in panel (a) indicate the average movement time $1/k_D$, rest time $1/k_E$, and motion-rest alternation process of $\sigma(t)$, while keys in panel (b) shows the average movement velocity V and evolution of the displacement for different values of $\sigma(t)$. Motion-rest alternation with velocity fluctuations produces tilted stair-step trajectories with unsteady slopes in the x–t plane.

as

$$\begin{aligned} \dot{x}(t) &= v(t)\sigma(t), \\ \dot{v}(t) &= [F(v)+\xi(t)]\sigma(t). \end{aligned} \tag{5}$$

Here, $F(u)$ is a deterministic force term whose structure can be chosen to produce the desired velocity distribution for moving particles (exponential, Gaussian, or others), $\xi(t)$ is a Gaussian white noise with correlation function

$$\langle \xi(t)\xi(t+\tau)\rangle = 2\Gamma\delta(\tau), \tag{6}$$

representing velocity fluctuations of moving particles, and Γ is a velocity diffusivity [units L^2/T^3] controlling the intensity of velocity fluctuations. Fig. (1) displays particle velocities and displacements derived from these equations for the choice of Gaussian movement velocities.

The quantity $\sigma(t)$ is a dichotomous Markov noise (e.g. Horsthemke and Lefever, 1984; Bena, 2006) which produces alternation between motion (generally nonzero velocity and acceleration) and rest (zero velocity and acceleration). This noise takes on values $\sigma = 1$ (motion) and $\sigma = 0$ (rest). The entrainment rate ($\sigma = 0 \to \sigma = 1$) is labeled k_E, and the deposition rate ($\sigma = 1 \to \sigma = 0$) is labeled k_D. Times spent in motion and rest are respectively distributed as $P(t) = k_D \exp(-k_D t)$ and $P(t) = k_E \exp(-k_E t)$, so the mean movement time is k_D^{-1}, and the mean resting time is k_E^{-1}. The notation $k = k_E + k_D$ is a shorthand used throughout the paper. $1/k$ represents the correlation time of the dichotomous noise.

Eq. (5) represents intermittent particle transport in an external force field. The transport is intermittent in that the velocity and acceleration are randomly switched on and off by entrainment and deposition. There are examples of similar systems in

https://doi.org/10.5194/esurf-2022-4
Preprint. Discussion started: 20 January 2022

the physics literature, although these involve just the velocity being switched between values, not the acceleration (e.g. Laskin, 1989; Łuczka et al., 1993; Balakrishnan et al., 2001). Thus we study a system which is “second order" in the dichotomous noise, which presents considerable mathematical challenges (e.g. Masoliver, 1993). To our knowledge, an analogue of Eq. (5) has not been examined.

2.2 Phase space description of motion-rest alternation

The time evolution of Eq. (5) for particular realizations of $\xi(t)$ and $\sigma(t)$ maps a trajectory through the phase space spanned by x and v. The conditional probability density $W(x,v,t|x_0,v_0)$ represents the likelihood that a phase trajectory reaches (x,v) at time t provided it passed through (x_0,v_0) at $t=0$. This density characterizes the stochastic evolution of the particle position and velocity.

A master equation for the phase space density can be formulated by noting that the combined process (x,v,σ) is Markovian (cf. Horsthemke and Lefever, 1984). In appendix A we demonstrate that Eq. (5) implies

$$\partial_t(\partial_t+k)W(x,v,t|0)=(\partial_t+k_E)\hat{L}_K W(x,v,t|0), \tag{7}$$

using the abbreviation $W(x,v,t|x_0,v_0)=W(x,v,t|0)$. In this equation, $\hat{L}_K$ is the *Kramers operator*, familiar from the description of Brownian particles in an external force field (e.g. Risken, 1984; Kubo et al., 1978):

$$\hat{L}_K=-v\partial_x+\partial_v\{-F(v)+\Gamma\partial_v\}. \tag{8}$$

To understand the structure of Eq. (7), it is useful to recall the classical Kramers equation for particles driven by a fluctuating force without intermittency: $\partial_t W(x,v,t|0)=\hat{L}_K W(x,v,t|0)$, with the same operator $\hat{L}_K$ as above (Kramers, 1940). A comparison suggests that the additional terms in Eq. (7) weave intermittency into the distribution function. In fact we can see as $k_D\to 0$ while $k_E\to\infty$, so that bedload particles immediately entrain and never deposit, Eq. (7) becomes the Kramers equation.

2.3 The displacement statistics of bedload grains

To calculate the sediment transport rate we will use the probability distribution of position for bedload particles, defined as

$$P(x,t|0)=\int_{-\infty}^{\infty}dv' W(x,v',t|0). \tag{9}$$

Unfortunately, even for the classical Kramers equation without intermittent motion, it is extremely difficult to obtain a governing equation for $P(x,t|0)$ without first solving the phase space master equation for $W(x,v,t|0)$ (e.g. Brinkman, 1956; Olivares-Robles and García-Colin, 1996). For the case of $F(v)$ associated with exponential velocities (e.g. Fan et al., 2014), the Kramers equation has only been solved numerically (Menzel and Goldenfeld, 2011).

Fortunately bedload experiments often show Gaussian velocities for moving particles (e.g. Martin et al., 2012; Ancey and Heyman, 2014; Heyman et al., 2016), corresponding to the forcing term

$$F(v)=\gamma(V-v). \tag{10}$$

https://doi.org/10.5194/esurf-2022-4
Preprint. Discussion started: 20 January 2022

With this force, the classical (non-intermittent) Kramers equation analogous to Eq. (7) can be exactly solved for the position distribution $P(x,t|0)$ (e.g. Wang and Uhlenbeck, 1945; Chandrasekhar, 1943). When motions are intermittent, corresponding to Eq. (7), an exact solution appears not yet possible.

We can however solve Eq. (7) with the force (10) approximately, by using the same "overdamped" approximation often applied to the classical Kramers equation (e.g. Risken, 1984; Gardiner, 1983). If we consider that moving particles attain their steady-state velocities relatively quickly after entrainment (i.e. the relaxation timescale $\gamma^{-1} \to 0$), we can actually obtain an overdamped approximation for the phase space equation (7) using the same method originally introduced by Kramers (1940).

We integrate Eq. (7) along the straight line $x + v\gamma^{-1} =$ const. from $v \to -\infty$ to $v \to \infty$. Because γ^{-1} is small, we can take the line integral along dv only (cf. Coffey et al., 2004), providing the overdamped master equation:

$$\left[\partial_t^2 + k\partial_t + V\partial_x\partial_t + k_E V\partial_x - D\partial_x^2\partial_t - k_E D\partial_x^2\right]P(x,t) = 0. \tag{11}$$

The spatial diffusivity D is defined as $D = \gamma^{-2}\Gamma$ with units $[L^2/T]$. Hereafter we suppress the explicit dependence of the position distribution on its initial conditions $[P(x,t|x_0,v_0,t_0) = P(x,t)]$.

Eq. (11) interleaves two different diffusion processes: one associated with motion-rest alternation, and another with velocity fluctuations during motions. We can see in particular that taking the entrainment rate k_E very large, meaning that particles are usually moving, implies the classical advection-diffusion equation $(\partial_t + V\partial_x - D\partial_x^2)P = 0$. This result is characteristic of a particle moving downstream with Gaussian velocity fluctuations. Otherwise, when k_D and k_E are comparable, there is a possibility that particle motions will be interrupted, giving rise to the additional terms in Eq. (11).

3 Mechanistic formulation of the sediment flux

Now we phrase the probability distribution of the sediment flux in terms of these particle dynamics. The method we present is very similar to the one developed by Banerjee et al. (2020) to describe current fluctuations in condensed matter physics. The basic idea, as depicted in Fig. (2), is to initially distribute N particles in all states of motion along the domain $-L \leq x \leq 0$. Later, the number of particles N and the size L of the domain will be extended to infinity such that their ratio $\rho = N/L$ remains constant. This limit produces a configuration similar to the one considered in the nonlocal formation of Eq. (3).

From this initial configuration, the flux is calculated as the average rate of particles crossing to the right of the control surface at $x = 0$ after the sampling time T, analogous to the renewal formulation of Eq. (4):

$$q(T) = \frac{1}{T}\sum_{i=1}^{N} I_i(T). \tag{12}$$

In this equation, the $I_i(T)$ are indicator functions which equal 1 if the ith particle has crossed the control surface ($x = 0$) by T, and 0 otherwise. Particles which have not crossed the surface (or which have crossed and then crossed back) do not contribute to the flux.

https://doi.org/10.5194/esurf-2022-4
Preprint. Discussion started: 20 January 2022

Earth Surface Dynamics
Discussions
Open Access

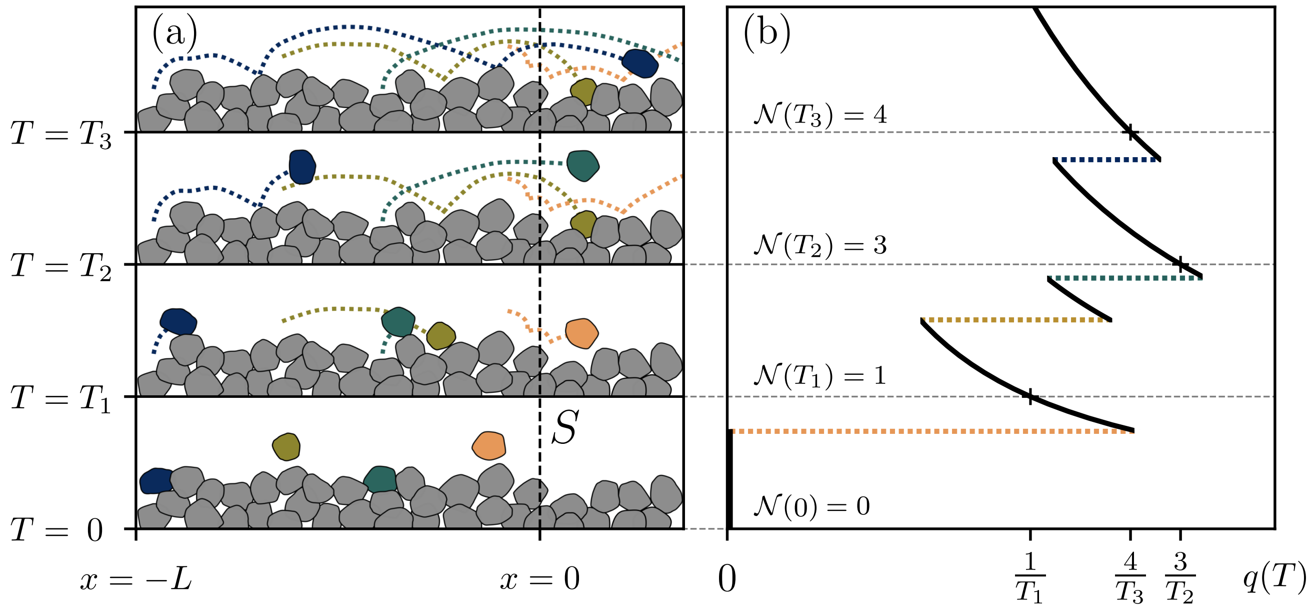

Figure 2. Panel (a) indicates the configuration for the flux. Here, time increases from the bottom to the top. Particles begin their transport with positions $-L \leq x \leq 0$ to the left of S at observation time $T = 0$, and the flux is calculated in panel (b) as the rate $\mathcal{N}(T)/T$ of particles crossing $x = 0$ over the observation time T. Particle crossing events are indicated in (b) by color-coded lines. The probability distribution of $q(T)$ is determined from all possible realizations of the trajectories and initial positions as N and L tend to infinity while the density of particles $\rho = N/L$ to the left of S is held constant.

The probability density $F(q|T)$ of the flux, conditional on the sampling time T, is then an average involving Eq. (12) across all possible initial configurations of particles and their trajectories:

165 $$F(q|T) = \left\langle \delta\left(q - \frac{1}{T}\sum_{i=1}^{N} I_i(T)\right)\right\rangle. \quad (13)$$

Taking the Laplace transform $\tilde{F}(s|T) = \int_0^\infty dq e^{-sq} F(q|T)$ (forming the characteristic function) produces

$$\tilde{F}(s|T) = \prod_{i=1}^{N}\left[1 - \left(1 - e^{-s/T}\right)\langle I_i(T)\rangle\right]. \quad (14)$$

This formula relies on the independence of averages for each particle (so that the average of a product is the product of averages) and the observation that $e^{\alpha I} = 1 - (1 - e^{\alpha})I$ if $I = 0, 1$.

https://doi.org/10.5194/esurf-2022-4
Preprint. Discussion started: 20 January 2022

The average over initial conditions and possible trajectories of the indicator for the ith particle involved in this characteristic function is

$$\langle I_i(T)\rangle = \frac{1}{L}\int_{-L}^{0} dx' \int_{0}^{\infty} dx P(x-x',T). \tag{15}$$

Here $P(x,T)$ is the position probability distribution of position at time T, either derived exactly from Eqs. (7) and (9), or from the overdamped approximation Eq. (11). The integral over x evaluates the probability that the position of a particle at T exceeds $x=0$, while the integral over x' averages across a uniform distribution of possible initial positions. These $\langle I_i(t)\rangle$ are the components of the flux that depend on the particle dynamics.

Inserting Eq. (15) into Eq. (14) and taking the limits $L\to\infty$ and $N\to\infty$, as the density of particles $\rho = N/L$ is held constant, provides

$$\tilde{F}(s|T) = \exp\Big[-\big(1-e^{-s/T}\big)\Lambda(T)\Big]. \tag{16}$$

$\Lambda(T)$ is the central parameter of the sediment flux probability distribution:

$$\Lambda(T) = \rho\int_{0}^{\infty} dx \int_{0}^{\infty} dx' P(x+x',T). \tag{17}$$

The quantity $\Lambda(T)/T$ is a *rate function*. This ratio describes the rate of particle arrivals to the control surface at $x=0$, and it explicitly depends on the observation time T.

Eq. (16) is the characteristic function of a Poisson distribution (Cox and Miller, 1965). Expanding in $e^{-s/T}$ and inverting the Laplace transforms provides the probability distribution of the flux conditional on the sampling time T:

$$F(q|T) = \sum_{n=0}^{\infty}\frac{\Lambda(T)^n}{n!}e^{-\Lambda(T)}\delta\big(q-\frac{n}{T}\big). \tag{18}$$

This equation implies that the mean flux is $\langle q(T)\rangle = \int_0^\infty qF(q|T)dq = \Lambda(T)/T$. Similarly the variance is $\sigma_q^2(T) = \Lambda(T)/T^2$. For the case when $\Lambda(T)$ is proportional to the observation time ($\Lambda\propto T$), these formulas become identical to the renewal approach with exponential inter-arrival times.

Eq. (18) formulates the flux probability distribution directly from the particle dynamics set out in Eq. (5). This equation is a scale-dependent Poisson distribution. The Poisson form originates primarily from the assumption that particles undergo independent dynamics. It is scale dependent through the displacement statistics of individual particles ingrained in Eq. (17).

4 Results

4.1 Displacement by intermittent transport

The overdamped master equation (11) describes the displacement statistics of particles alternating between motion and rest with Gaussian movement velocities. This equation is founded on the approximation that just-entrained particles attain their steady-state (but fluctuating) velocities rapidly.

https://doi.org/10.5194/esurf-2022-4
Preprint. Discussion started: 20 January 2022

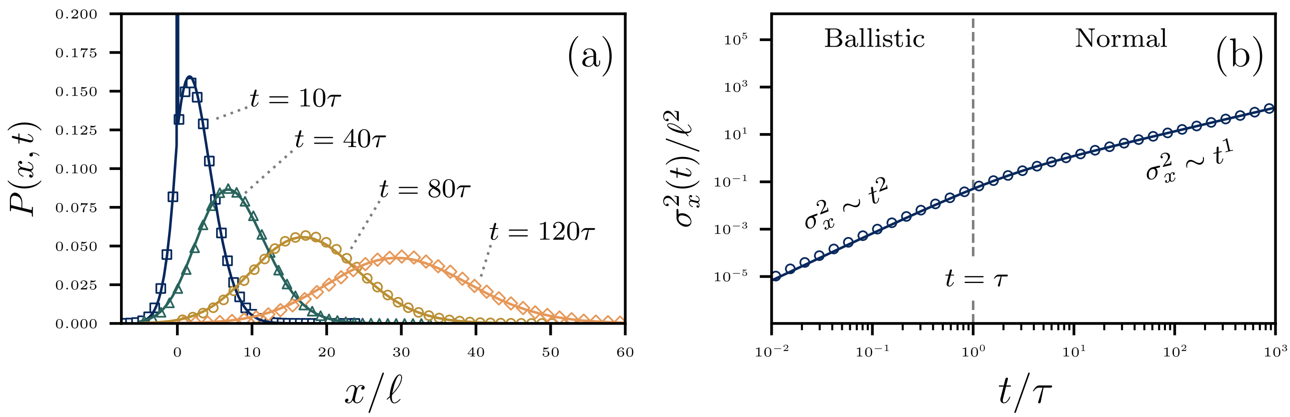

Figure 3. Panel (a) indicates the overdamped probability distribution of particle position (19) as it evolves through time, while panel (b) shows the resulting particle diffusion from Eq. (20). All results are scaled by the mean hop length $\ell = V/k_D$ and the timescale $\tau = 1/k$ of the motion-rest alternation. Curves represent the analytical results while the points are results of Monte Carlo simulations of the exact equations (5) produced by evaluating the cumulative transition probabilities on a small timestep (e.g. Barik et al., 2006). In panel (a) from the initial mixture of motion and rest states, particles advect downstream as they diffuse apart from one another due to motion-rest alternation and velocity variations. The initial distribution persists as a delta function spike for the $t = 10\tau$ curve. In panel (b) at timescales $t \ll 1/k$ the diffusion is approximately ballistic since particles have not had time to exchange between motion and rest. For $t \gg 1/k$ particles undergo normal diffusion as particles become well-mixed among motion and rest states. Small discrepancies are visible at short times between the simulations and analytical approximations due to our neglect of velocity fluctuations in deriving Eq. (20).

The overdamped master equation (11) is solved in appendix B with transform calculus, obtaining

$$P(x,t) = \hat{A} \int_0^t e^{-k_E(t-u)-k_D u} \mathcal{I}_0\left(2\sqrt{k_E k_D u(t-u)}\right) \frac{e^{-(x-Vu)^2/4Du}}{\sqrt{4\pi D u}} du. \tag{19}$$

Here $\mathcal{I}_0$ is a modified Bessel function and $\hat{A} = -D\partial_x^2 + V\varphi\partial_x + k + \partial_t$ is a differential operator. Within the integral, the Bessel term represents the proportion of time u/t the particle has spent in motion, while the Gaussian term describes the distribution of displacements achieved in time u. This distribution is compared with numerical simulations of the exact distribution from Eq. (5) in Fig. (3)a. The general decreasing trend of mean transport with observation time is qualitatively consistent with laboratory observations (Singh et al., 2009; Saletti et al., 2015) and the renewal approach summarized earlier (Turowski, 2010; Ancey and Pascal, 2020).

The moments of particle position from Eq. (5) are extremely challenging to obtain. An approximation for the mean can be obtained by considering that velocity fluctuations during motions approximately cancel out, since these are symmetrical around V. Therefore we set $\Gamma = 0$ in Eq. (5) to find the mean position $\langle x(t)\rangle = k_E V t/k$, which is Vt scaled by the expected fraction of time spent in motion. Similarly we can approximate the variance by reasoning that motion-rest alternation, and not velocity fluctuations during motions, is the primary source of particle diffusion. Again setting $\Gamma = 0$ we find the variance of position

https://doi.org/10.5194/esurf-2022-4
Preprint. Discussion started: 20 January 2022

Earth Surface Dynamics Discussions

($\sigma_x^2 = \langle x^2 \rangle - \langle x \rangle^2$):

$$\sigma_x(t)^2 = \frac{2k_E k_D V^2}{k^3}\Big(t + \frac{1}{k}e^{-kt} - \frac{1}{k}\Big). \tag{20}$$

This describes a two-range particle diffusion process, whereby the rate of particle spreading depends on how long the dynamics have been ongoing (Taylor, 1920). Fig. (3)b compares this variance to the numerical solutions and exhibits a crossover between ballistic and normal scaling regimes at $\tau = 1/k$. The variance approximation is good apart from small undershooting at short times. Here, small contributions to the variance from velocity fluctuations in the motion state become visible, suggesting that particle velocity fluctuations during motions slow the diffusion at short timescales.

4.2 The flux rate function for overdamped transport

The formalism in Sec. 3 provides the central parameter $\Lambda(T)$ of the sediment flux distribution. Using the overdamped probability distribution of position Eq. (19), we evaluate Eq. (17) in appendix C, providing

$$\Lambda(T) = \rho \int_0^T \mathcal{I}_0\Big(2\sqrt{k_E k_D u(T-u)}\Big)e^{-k_E(T-u)-k_D u} \times \left[\sqrt{\frac{D}{\pi u}}\Big([\overleftarrow{\partial}_T + k]u - \frac{k_D}{2k}\Big)e^{-V^2u/4D} + \frac{V}{2}\Big([\overleftarrow{\partial}_T + k]u - \frac{k_D}{k}\Big)\operatorname{erfc}\left(-\sqrt{\frac{V^2u}{4D}}\right)\right]du. \tag{21}$$

In this equation, the notation $\overleftarrow{\partial}_T$ means that the partial time derivative acts from the left of all terms in which it is involved, as in $f(T)\overleftarrow{\partial}_T g(T) = \partial_T[f(T)g(T)]$, and $\operatorname{erfc}(x)$ denotes the complementary error function.

This result indicates a nuanced observation-scale dependence in the sediment flux. We can better understand Eq. (21) by investigating extreme cases of the observation time. As shown in appendix D, Eq. (21) takes on simple forms at extreme values of T:

$$\Lambda(T) = \begin{cases} \frac{\rho k_E}{k}\sqrt{\frac{DT}{\pi}}, & T \ll (k_D Pe)^{-1}, \\ \frac{\rho k_E V T}{k}, & T \gg (k_D Pe)^{-1}. \end{cases} \tag{22}$$

Here, $Pe = V^2/(2Dk_D)$ is a Péclet number that measures the relative importance of advection and diffusion to the particle motion.

The limiting form of $\Lambda(T)$ implies that for $T \gg (k_D Pe)^{-1}$ the mean flux converges to the eventual value $\langle q(T \to \infty)\rangle = q_0$:

$$q_0 = \rho k_E V/k. \tag{23}$$

This can be understood as the result $q_0 = E\ell$ of the nonlocal formulation (3) in the case of steady transport conditions. Thus at $T \to \infty$ our formlation becomes equivalent to that of Einstein (1950). Here, $E = \rho k_E$ is an averaged areal entrainment rate and $\ell = V/k \approx V/k_D$ is the mean step length of particles. $k \approx k_D$ holds since the mean duration of a single motion is typically much smaller than the duration of a single rest.

Fig. (4)a shows the rate constant decaying toward its asymptotic value in Eq. (22) for different values of *Pe*. Numerical simulations of the exact equations (5) are superimposed. The overdamped approximation pursued in this paper provides a valid characterization of the sediment flux for $T \gg 1/\gamma$, but for $T \ll 1/\gamma$, the approximate result overshoots. Thus in general we expect the properties of particle acceleration immediately after entrainment (cf. Campagnol et al., 2015) will slow the observation-scale dependence of the flux at short timescales.

Fig. (4)b demonstrates the adjustment of the flux distribution (12) across observation times. At the shortest times, the flux approaches a uniform-like distribution due to the (apparent) divergence of $\Lambda(T)$. At very long observation times, the flux adopts the deterministic (Einstein) form

$$F(q|T) \sim \delta(q - E\ell). \tag{24}$$

This limit can be seen by taking large T in Eq. (18) and using the correspondence between Poisson and Gaussian distributions for large Poisson rates (e.g. Cox and Miller, 1965). The Einstein (1950) result for the sediment transport rate becomes exact in the limit the observation is large compared to the key timescale $1/k$ of motion-rest alternation. Otherwise, the flux has intrinsic fluctuations related to the unpredictability of particle arrivals in a finite observation window, as characterized by Eq. (12).

5 Discussion

In this paper, we formulated a mechanistic description of the bedload sediment flux using a detailed stochastic model of individual particle displacements. The resulting sediment flux distribution shows Poissonian fluctuations that depend on observation scale. Our displacement model applies over a wider range of timescales than earlier formulations because it includes both Newtonian velocities and motion-rest alternation. In appropriate simplified limits, the displacement model Eq. (7) reduces to many earlier descriptions of grain-scale transport (e.g. Einstein, 1937; Lisle et al., 1998; Lajeunesse et al., 2017; Ancey and Heyman, 2014; Fan et al., 2014). In this sense, the grain-scale transport component of this paper generalizes and unifies all of these earlier works.

We solved the displacement model analytically to obtain the displacement probability distribution. This derivation relied on the “overdamped" approximation that particles accelerate rapidly following entrainment. We then formulated the stochastic sediment flux using the resulting particle displacement statistics. The obtained flux distribution mimics earlier renewal theory descriptions of the bedload flux (Turowski, 2010; Ancey and Pascal, 2020), except its input parameters relate directly to the transport characteristics of individual grains. The flux distribution depends on the timescale over which it is observed. It inherits this scale-dependence from the velocity fluctutations and motion-rest alternations of individual grains. The convergence timescale of the flux indicates this conclusion: transport rates converge for timescales $T = (k_D Pe)^{-1}$. The convergence thus links to the deposition rate of individual particles (inverse time spent in motion) and the Péclet number which measures the significance of movement velocity fluctuations. When the time spent in motion goes to zero (idealized steps), or velocity fluctuations vanish ($Pe \to \infty$), the flux loses its scale dependence. In other conditions, the flux approaches the deterministic result $q = E\ell$ of Einstein (1950) and later nonlocal formulations (Furbish et al., 2012, 2017) as the observation time becomes large.

https://doi.org/10.5194/esurf-2022-4
Preprint. Discussion started: 20 January 2022

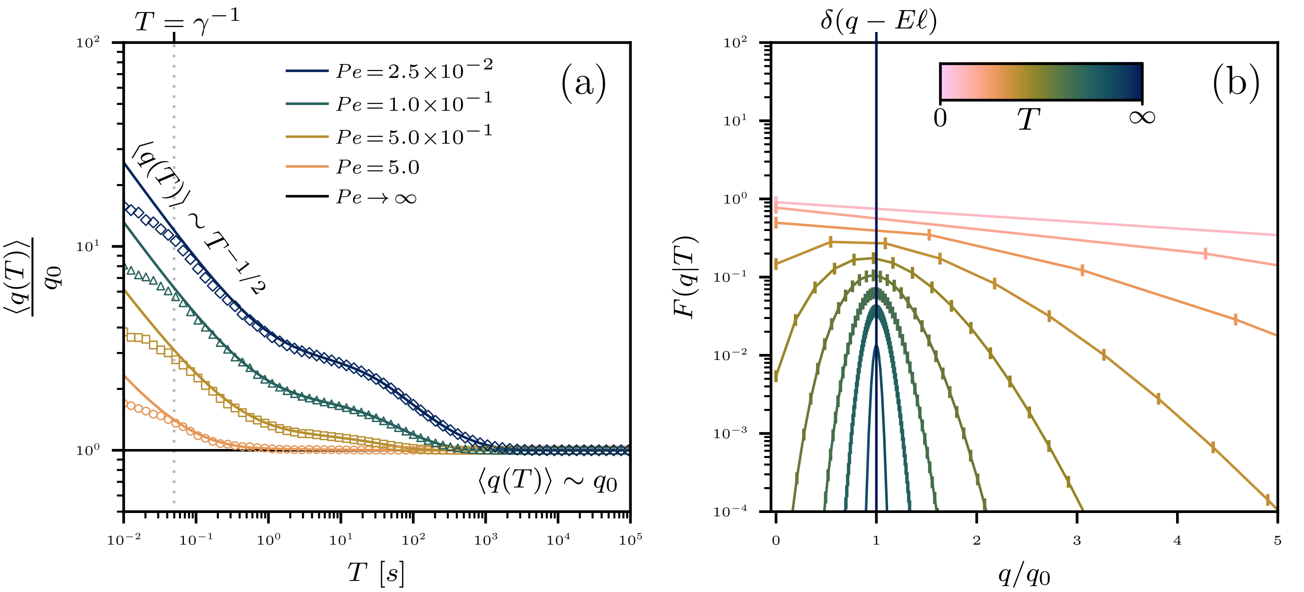

Figure 4. Panel (a) plots the mean sediment flux for different values of the Péclet number $Pe = V^2/(2k_D D)$, characterizing the relative significance of particle velocity fluctuations during motion. Plotted lines show the analytical result (21), while the points are Monte Carlo simulations. Panel (b) displays the evolution of the flux distribution (18) across observation times. The flux is normalized by the prediction $q_0 = E\ell$ of the Einstein model. In panel (a), the convergence time of the mean flux is controlled by attributes of individual particle motions. In all cases, the mean flux converges for $T \gg 1/(k_D Pe)$, as expected by Eq. (22). The overdamped approximation (22) cannot account for timescales $T \ll \gamma^{-1}$, as indicated by the discrepancy between numerical and analytical calculations. In panel (b), the Einstein limit $F(q|T) = \delta(q - E\ell)$ is approached as the observation time T grows. Stronger velocity fluctuations (smaller *Pe*) slow the convergence.

5.1 Newtonian description of bedload displacement

Our description of individual particle displacements in Sec. 2 provides an analytically-solvable alternative to computational-physics models of grain-scale transport (e.g. Schmeeckle, 2014; Ji et al., 2014; Clark et al., 2017). Analytical progress was possible largely because the forces on moving particles were modeled as linear in the particle velocity [Eq. (10)] with Gaussian white noise fluctuations (cf. Ancey and Heyman, 2014). This forcing structure is a crude approximation for the actual hydrodynamic and granular forces acting on bedload particles. In reality, flow forces are non-linear in the flow velocity and history-dependent (Michaelides, 1997; Schmeeckle et al., 2007), while collision forces are velocity-dependent and episodic (Brach, 1989; Schmeeckle and Nelson, 2003; Pierce, 2021). Fluctuations in these forces are probably *colored* noise, not white (Hänggi and Jung, 2007; Cameron et al., 2020). Although we cannot hope to include completely realistic forces into an analytically-solvable model, it should still be possible to introduce some level of additional complexity into the forcing structure of Eq. (5). A first step is to solve Eq. (7) with $F(v)$ tailored to produce exponential velocities for moving particles (e.g. Fan et al., 2014). The result would lend additional insight into how the scale-dependence of the flux depends on the particle velocity statistics.

https://doi.org/10.5194/esurf-2022-4
Preprint. Discussion started: 20 January 2022

A simplified element of our approach is the representation of entrainment and deposition by instantaneous alternation between motion and rest states (e.g. Einstein, 1937). In actuality, motion and rest are not perfectly defined because "resting" particles undergo slow downstream creep (Houssais et al., 2015; Allen and Kudrolli, 2018) and can shuttle in their pockets without any net translation (Diplas et al., 2008; Celik et al., 2010). It is challenging to imagine an analytically-solvable model of particle displacement which does not discriminate between multiple states of transport, but improvements can nonetheless be made to the dichotomous representation of entrainment and deposition we employed. One option is to render slower-moving particles more likely to deposit, which can be viewed as making the dichotomous noise "state dependent" (e.g. Laio et al., 2008; Bartlett and Porporato, 2018). This would preferentially cull slow-moving particles and positively skew the particle velocity distribution among moving particles (Williams and Furbish, 2021), possibly affecting the sediment flux.

5.2 Mechanistic interpretation of transport fluctuations

The sediment flux probability distribution derived in Sec. 3 represents a Poisson distribution with a scale-dependent rate. Poisson distributions have relatively thin tails which reflect narrow sediment transport fluctuations. In reality, sediment flux distributions are only Poissonian at high transport rates, whereas in other conditions they have wide tails representing the possibility of large fluctuations (Ancey et al., 2008; Saletti et al., 2015; Turowski, 2010), which appear as bursts (e.g. Goh and Barabási, 2008) in sediment flux timeseries (Dhont and Ancey, 2018; Singh et al., 2009). This observation highlights a need to improve the mechanistic description we developed here to produce wider transport rate fluctuations.

A vast set of processes generate transport rate fluctuations in real channels. At the shortest timescales, fluctuations arise from the intermittent arrivals of individual grains, as we have described here. Over longer timescales, activity waves (Heyman et al., 2014), cluster entrainment (Papanicolaou et al., 2018; Strom et al., 2004), bedform migration (Guala et al., 2014; Hamamori, 1962), grain-size sorting (Cudden and Hoey, 2003; Iseya and Ikeda, 1987), flow variations (Mao, 2012; Wong and Parker, 2006), and sediment supply perturbations (Lisle et al., 1993; Madej et al., 2009) all contribute to sediment transport variability. It should be possible to include particle-particle interactions into our description to capture the subset of these processes which originate from the grain-scale physics. Activity waves, clusters, and bedforms might result from including interactions between particles into the entrainment and deposition rates, such as collisions (Lee and Jerolmack, 2018), the stabilization of bed particles by neighbors, or coordinated deposition based on the locations of sedimentary deposits (cf. McDowell and Hassan, 2020). We might formulate the resulting joint distribution of particle positions and velocities by analogy to reaction-diffusion problems (e.g. Pechenik and Levine, 1999; Cardy, 2008) or other interacting particle systems available in the physics literature (e.g. Escaff et al., 2018; Hernández-García and López, 2004).

5.3 Observation-scale dependence of the flux distribution

The observation-scale dependence of the sediment flux has been investigated in several laboratory experiments. Both Singh et al. (2009) and Saletti et al. (2015) found that the statistical moments of the bedload flux shift with the observation time T, but Singh et al. identified statistical *multiscaling*, where the flux distribution changes shape with T, while Saletti et al. identified *monoscaling*, where the distribution does not change shape with T. Our approach predicts monoscaling because

https://doi.org/10.5194/esurf-2022-4
Preprint. Discussion started: 20 January 2022

the flux distribution (18) is always Poissonian, even though all of its moments scale together with T in a non-trivial way, see Fig. (4). Probably the Poissonian and monoscaling characteristics of the flux distribution both originate from the assumed independence of individual particle motions which was used to arrive at Eq. (16). Turowski (2010) demonstrated that renewal theories with certain non-exponential inter-arrival times produce multiscaling. Possibly, wider-tailed, multiscaling sediment flux distributions will derive from generalizations of our approach to include particle-particle interactions. To some extent a flux distribution which is wide-tailed at short observation times *must* be multiscaling, since it should approach the thin-tailed (deterministic) Einstein distribution (24) as the observation time becomes large, changing shape as it adjusts.

6 Conclusions

We have formulated the bedload flux probability distribution using the statistical mechanics of individual grains in transport. This formulation produces Poissonian flux distributions having scale-dependent rates, meaning transport rate fluctuations are relatively narrow, and transport characteristics shift with the timescales over which they are observed. In laboratory experiments, sediment transport fluctuations are typically wider than Poissonian. Notably, we can assert that the Poisson flux distribution derived in this paper originates exclusively from the independence of individual grains: the Poisson form is completely indifferent to the forces driving particles downstream, so long as these forces do not introduce correlations between particles. In the future it will be necessary to refine the statistical mechanics formulation presented here to produce wider transport fluctuations. We expect that introducing any component in Eq. (5) which couples one particle to another will achieve wider flux distributions than Poisson. The severe challenge will be evaluating the average in Eq. (14) when grains are not independent.

Appendix A: Derivation of the phase space master equation

Because the joint process (x,v,σ) is Markovian, its phase space distribution function for a particular realization of the white noise $\xi(t)$ obeys the Chapman-Kolmogorov equation (Cox and Miller, 1965; Van Kampen, 2007):

$$W_\xi(x,v,\sigma,t+\delta t|x_0,v_0,\sigma_0,t_0) = \sum_{\sigma'=0,1} \int_{-\infty}^{\infty} dx' \int_{-\infty}^{\infty} dv' W_\xi(x,v,\sigma,t+\delta t|x',v',\sigma',t) W_\xi(x',v',\sigma',t|x_0,v_0,\sigma_0,t_0). \tag{A1}$$

This equation relates the phase space distribution function at $t+\delta t$ to its value at t through the transition amplitudes $W_\xi(x,v,\sigma,t+\delta t|x',v',\sigma',t)$. The distribution W_ξ is a *functional* of the white noise $\xi(t)$ (Hänggi, 1985; Łuczka, 2005).

In the limit of vanishing δt, the transition amplitudes in Eq. (A1) can be directly evaluated from the dynamical equations Eq. (5) using a method analogous to Horsthemke and Lefever (1984). The transition rates involve δ-function terms in x' and v'. These terms are expanded in δt to first order, and the integrals in Eq. (A1) are conducted over the δ-functions. This produces the pair of equations

$$\begin{aligned} \partial_t M_\xi &= k_E R_\xi - k_D M_\xi + \big\{ -\partial_x v + \partial_v [-F(v) + \xi(t)] \big\} M_\xi \\ \partial_t R_\xi &= k_D M_\xi - k_E R_\xi. \end{aligned} \tag{A2}$$

https://doi.org/10.5194/esurf-2022-4
Preprint. Discussion started: 20 January 2022

In these equations the shorthands are $M_\xi = W_\xi(x,v,1,t|x_0,v_0,\sigma_0,t_0)$ and $R_\xi = W_\xi(x,v,0,t|x_0,v_0,\sigma_0,t_0)$. We now average Eq. (A2) over realizations of the white noise and compute the correlator $\langle \xi(t) M_\xi \rangle = \Gamma \partial_v M$ using the Furutsu-Novikov theorem (e.g. Van Kampen, 2007; Gitterman, 2005). Incorporating this correlator into Eq. (A2) obtains

$$\begin{aligned} \partial_t M &= k_E R - k_D M + L_K M \\ \partial_t R &= k_D M - k_E R, \end{aligned} \tag{A3}$$

where $\hat{L}_K = -\partial_x v + \partial_v\{-F(v) + \Gamma\partial_v\}$ is the Kramers operator, $M = \langle M_\xi \rangle$, and $R = \langle R_\xi \rangle$. Summing the above equations, noting $W(x,v,t|0) = M + R$, and eliminating M from the sum produces Eq. (7).

Appendix B: Solution for the position probability distribution

The position probability distribution can be obtained from Eq. (11) provided we have a pair of initial conditions on P. We consider that particles have a probability $k_D/k = \varphi$ to start from rest, so they have a probability $1-\varphi = k_E/k$ to start from motion. Particles are initially located at $x = 0$, and particles that start from motion are considered to have a random initial velocity selected from the steady-state distribution

$$f(v) = \sqrt{\frac{\gamma}{2\pi\Gamma}} e^{-\gamma v^2/2\Gamma}. \tag{B1}$$

With these assumptions, the initial state can be written $M(x,v,0) = (1-\varphi)\delta(x)f(v)$ and $R(x,v,0) = \varphi\delta(x)\delta(v)$. Summing these two equations and integrating out the velocity provides $P(x,0) = \delta(x)$. Plugging these two equations into Eq. (A3), summing the result, then integrating out the velocity provides $\partial_t P(x,0) = -\frac{k_E V}{k}\delta'(x)$. This produces the required pair of initial conditions. A similar calculation is available in Weiss (2002).

Now we take Fourier transforms over space and Laplace transforms over time of the overdamped master equation (11), obtaining

$$\tilde{\bar{P}}(g,s) = \frac{s + k + Dg^2 - igV\varphi}{s(s+k) + (Dg^2 - igV)(s+k_E)}. \tag{B2}$$

The Fourier transform can be inverted by partial fraction decomposition and contour integration to obtain

$$\tilde{P}(x,s) = \frac{-\varphi D\partial_x^2 + V\varphi\partial_x + s + k}{VR(s+k_E)} \exp\left[\frac{Vx}{2D} - \frac{V|x|}{2D}R\right], \tag{B3}$$

where

$$R = \sqrt{1 + \frac{4D}{V^2}\frac{s(s+k)}{s+k_E}}. \tag{B4}$$

The Laplace transform can then be inverted with the shift property $\mathcal{L}^{-1}\{\tilde{f}(s+k)\} = e^{-kt}f(t)$, the derivative property (Arfken, 1985)

$$\mathcal{L}^{-1}\{s\tilde{f}\} = (\delta(t) + \partial_t)f(t), \tag{B5}$$

https://doi.org/10.5194/esurf-2022-4
Preprint. Discussion started: 20 January 2022

the identity (Bateman and Erdelyi, 1953, pg. 133)

$$\mathcal{L}^{-1}\left\{\frac{1}{s}\tilde{g}(s-a/s)\right\}=\int_0^t \mathcal{I}_0\left(2\sqrt{au(t-u)}\right)g(u)du, \tag{B6}$$

and Laplace transform tables (Prudnikov et al., 1992), eventually giving Eq. (19).

Appendix C: Calculation of the scale-dependent rate function

The Laplace transform of Eq. (17) over T provides

$$\tilde{\Lambda}(s)=\rho\int_0^\infty dx_i\int_0^\infty dx\tilde{P}(x+x_i,s). \tag{C1}$$

Noting that $x+x_i$ is always positive, inserting Eq. (19), and integrating twice gives

$$\tilde{\Lambda}(s)=-\frac{\rho\varphi D}{VR(s+k_E)}+\frac{2\rho D\varphi}{VR(1-R)(s+k_E)}+\frac{4\rho D^2(s+k)}{V^3R(1-R)^2(s+k_E)}. \tag{C2}$$

Taking the inverse transform, applying Eq. (B5), and using the shift property develops

$$\Lambda(T)=\rho e^{-k_ET}\mathcal{L}^{-1}\left\{-\frac{\varphi D}{VR_\star s}+\frac{2D\varphi}{VR_*(1-R_\star)s}+\frac{4D^2\left(\overleftarrow{\partial}_T+k\right)}{V^3R_\star(1-R_\star)^2s}\right\}. \tag{C3}$$

Here, the notation $\overleftarrow{\partial}_T$ means the derivative acts from the left on all terms multiplying it, and

$$R_*=\sqrt{1+\frac{4D(k_D-k_E)}{V^2}+\frac{4D}{V^2}\left(s-\frac{k_Ek_D}{s}\right)}. \tag{C4}$$

Laplace inverting Eq. (C3) with Eq. (B6) and tabulated Laplace transforms (e.g. Arfken, 1985; Prudnikov et al., 1992) eventually provides Eq. (21).

Appendix D: Asymptotic limits of the flux rate function

The behavior of Eq. (21) at extreme values of T can be obtained with Tauberian theorems by inverting the Laplace-transformed rate function (C2) at the opposite extreme of s (Weiss, 1994). At short times, expanding Eq. (C2) as $s\to\infty$ gives

$$\tilde{\Lambda}(s)=\frac{\rho k_EV}{2ks^2}+\frac{\rho k_E}{k}\sqrt{\frac{D}{4s^3}}, \tag{D1}$$

which inverts to

$$\Lambda(t)\sim\frac{\rho k_EVT}{2k}+\frac{\rho k_E}{k}\sqrt{\frac{DT}{\pi}}, \tag{D2}$$

Earth Surface Dynamics Discussions Open Access EGU

giving the small T behavior. This has two scaling limits within it. Provided that $T \ll 4D/(V^2\pi) < 2D/V^2$, the scaling goes as $\Lambda(T) \sim T^{-1/2}$. But if $T \gg 2D/V^2$, it goes as $\Lambda(t) \sim T$. For large times, taking $s \to 0$ gives

$$\tilde{\Lambda}(s) = \frac{\rho k_E V}{ks^2}, \tag{D3}$$

and this inverts to $\Lambda(T) = \rho k_E VT/k$. These limits are summarized in Eq. (22).

Code availability. Python scripts for Monte Carlo simulation and to develop are available temporarily at https://github.com/jkpierce/flippyflop. The scripts contain comments detailing the stochastic simulation methods. This code will later be moved to a location with a DOI.

Author contributions. KP performed all calculations and constructed all figures. All authors (KP, MH, and RF) contributed equally to manuscript preparation.

Competing interests. We declare no competing interests.

https://doi.org/10.5194/esurf-2022-4
Preprint. Discussion started: 20 January 2022

Earth Surface Dynamics Discussions

References

Allen, B. and Kudrolli, A.: Granular bed consolidation, creep, and armoring under subcritical fluid flow, Physical Review Fluids, 7, 1–13, https://doi.org/10.1103/PhysRevFluids.3.074305, 2018.

Ancey, C. and Heyman, J.: A microstructural approach to bed load transport: Mean behaviour and fluctuations of particle transport rates, Journal of Fluid Mechanics, 744, 129–168, https://doi.org/10.1017/jfm.2014.74, 2014.

Ancey, C. and Pascal, I.: Estimating mean bedload transport rates and their uncertainty, Journal of Geophysical Research: Earth Surface, 125, 1–29, https://doi.org/10.1029/2020JF005534, 2020.

Ancey, C., Böhm, T., Jodeau, M., and Frey, P.: Statistical description of sediment transport experiments, Physical Review E, 74, 1–14, https://doi.org/10.1103/PhysRevE.74.011302, 2006.

Ancey, C., Davison, A. C., Böhm, T., Jodeau, M., and Frey, P.: Entrainment and motion of coarse particles in a shallow water stream down a steep slope, Journal of Fluid Mechanics, 595, 83–114, https://doi.org/10.1017/S0022112007008774, 2008.

Arfken, G.: Mathematical Methods for Physicists, Academic Press, Inc., San Diego, https://doi.org/10.1063/1.3062258, 1985.

Bagnold, R. A.: An approach to the sediment transport problem from general physics, Tech. Rep. 4, U.S. Geological Survey, Washington, DC, https://doi.org/10.1017/s0016756800049074, 1966.

Balakrishnan, V., Van Den Broeck, C., and Bena, I.: Stochastically Perturbed Flows: Delayed and Interrupted Evolution, Stochastics and Dynamics, 01, 537–551, https://doi.org/10.1142/s0219493701000230, 2001.

Ballio, F., Nikora, V., and Coleman, S. E.: On the definition of solid discharge in hydro-environment research and applications, Journal of Hydraulic Research, 52, 173–184, https://doi.org/10.1080/00221686.2013.869267, 2014.

Ballio, F., Pokrajac, D., Radice, A., and Hosseini Sadabadi, S. A.: Lagrangian and Eulerian description of bed load transport, Journal of Geophysical Research: Earth Surface, 123, 384–408, https://doi.org/10.1002/2016JF004087, 2018.

Banerjee, T., Majumdar, S. N., Rosso, A., and Schehr, G.: Current fluctuations in noninteracting run-and-tumble particles in one dimension, Physical Review E, 101, 1–16, https://doi.org/10.1103/PhysRevE.101.052101, 2020.

Barik, D., Ghosh, P. K., and Ray, D. S.: Langevin dynamics with dichotomous noise; Direct simulation and applications, Journal of Statistical Mechanics: Theory and Experiment, https://doi.org/10.1088/1742-5468/2006/03/P03010, 2006.

Bartlett, M. S. and Porporato, A.: State-dependent jump processes: Itô-Stratonovich interpretations, potential, and transient solutions, Physical Review E, 98, 1–16, https://doi.org/10.1103/PhysRevE.98.052132, 2018.

Bateman, H. and Erdelyi, A.: Higher Transcendental Functions, McGraw-Hill, New York, 1953.

Bena, I.: Dichotomous Markov noise: Exact results for out-of-equilibrium systems, International Journal of Modern Physics B, 20, 2825–2888, https://doi.org/10.1142/S0217979206034881, 2006.

Böhm, T., Ancey, C., Frey, P., Reboud, J. L., and Ducottet, C.: Fluctuations of the solid discharge of gravity-driven particle flows in a turbulent stream, Physical Review E, 69, 13, https://doi.org/10.1103/PhysRevE.69.061307, 2004.

Brach, R. M.: Rigid body collisions, American Society of Mechanical Engineers, 56, 133–138, 1989.

Brilliantov, N. V. and Poschel, T.: Kinetic Theory of Granular Gases, Oxford University Press, Oxford, 1st edn., 2004.

Brinkman, H. C.: Brownian motion in a field of force and the diffusion theory of chemical reactions, Physica, 22, 149–155, https://doi.org/10.1016/S0031-8914(56)80019-0, 1956.

Bunte, K. and Abt, S. R.: Effect of sampling time on measured gravel bed load transport rates in a coarse-bedded stream, Water Resources Research, 41, 1–12, https://doi.org/10.1029/2004WR003880, 2005.

Cameron, S. M., Nikora, V. I., and Witz, M. J.: Entrainment of sediment particles by very large-scale motions, Journal of Fluid Mechanics, 888, https://doi.org/10.1017/jfm.2020.24, 2020.

Campagnol, J., Radice, A., Ballio, F., and Nikora, V.: Particle motion and diffusion at weak bed load: Accounting for unsteadiness effects of entrainment and disentrainment, Journal of Hydraulic Research, 53, 633–648, https://doi.org/10.1080/00221686.2015.1085920, 2015.

Cardy, J.: Reaction-diffusion processes, in: Non-Equilibrium Statistical Physics and Turbulence, edited by Nazarenko, S. and Zaboronski, O. V., pp. 108–161, Cambridge University Press, Cambridge, 2008.

Celik, A. O., Diplas, P., Dancey, C. L., and Valyrakis, M.: Impulse and particle dislodgement under turbulent flow conditions, Physics of Fluids, 22, 1–13, https://doi.org/10.1063/1.3385433, 2010.

Chandrasekhar, S.: Stochastic problems in physics and astronomy, https://doi.org/10.1103/RevModPhys.15.1, 1943.

Church, M.: Bed material transport and the morphology of alluvial river channels, Annual Review of Earth and Planetary Sciences, 34, 325–354, https://doi.org/10.1146/annurev.earth.33.092203.122721, 2006.

Clark, A. H., Shattuck, M. D., Ouellette, N. T., and O'Hern, C. S.: Role of grain dynamics in determining the onset of sediment transport, Physical Review Fluids, 2, https://doi.org/10.1103/PhysRevFluids.2.034305, 2017.

Coffey, W., Kalmykov, Y., and Waldron, J.: The Langevin equation, World Scientific, London, 1st edn., https://doi.org/10.1016/j.crhy.2017.10.001, 2004.

Cox, D. R. and Miller, H. D.: The Theory of Stochastic Processes, Wiley, New York, 1965.

Cudden, J. R. and Hoey, T. B.: The causes of bedload pulses in a gravel channel: The implications of bedload grain-size distributions, Earth Surface Processes and Landforms, 28, 1411–1428, https://doi.org/10.1002/esp.521, 2003.

Dhont, B. and Ancey, C.: Are bedload transport pulses in gravel bed rivers created by bar migration or sediment waves?, Geophysical Research Letters, 45, 5501–5508, https://doi.org/10.1029/2018GL077792, 2018.

Diplas, P., Dancey, C. L., Celik, A. O., Valyrakis, M., Greer, K., and Akar, T.: The role of impulse on the initiation of particle movement under turbulent flow conditions, Science, 322, 717–720, https://doi.org/10.1126/science.1158954, 2008.

Einstein, H. A.: Bed load transport as a probability problem, Ph.D. thesis, ETH Zurich, citeulike-article-id:12275990, 1937.

Einstein, H. A.: The bedload function for sediment transportation in open channel flows, Tech. rep., United States Department of Agriculture, Washington, DC, http://www.ncbi.nlm.nih.gov/pubmed/3333789, 1950.

Escaff, D., Toral, R., Van Den Broeck, C., and Lindenberg, K.: A continuous-time persistent random walk model for flocking, Chaos, 28, 1–11, https://doi.org/10.1063/1.5027734, 2018.

Fan, N., Zhong, D., Wu, B., Foufoula-Georgiou, E., and Guala, M.: A mechanistic-stochastic formulation of bed load particle motions: From individual particle forces to the Fokker-Planck equation under low transport rates, Journal of Geophysical Research: Earth Surface, 119, 464–482, https://doi.org/10.1002/2013JF002823, 2014.

Fathel, S. L., Furbish, D. J., and Schmeeckle, M. W.: Experimental evidence of statistical ensemble behavior in bed load sediment transport, Journal of Geophysical Research: Earth Surface, 120, 2298–2317, https://doi.org/10.1002/2015JF003552, 2015.

Furbish, D. J., Ball, A. E., and Schmeeckle, M. W.: A probabilistic description of the bed load sediment flux: 4. Fickian diffusion at low transport rates, Journal of Geophysical Research: Earth Surface, 117, 1–13, https://doi.org/10.1029/2012JF002356, 2012.

Furbish, D. J., Fathel, S. L., and Schmeeckle, M. W.: Particle motions and bedload theory: The entrainment forms of the flux and the Exner equation, in: Gravel-Bed Rivers: Process and Disasters, edited by Tsutsumi, D. and Laronne, J. B., chap. 4, pp. 97–120, John Wiley & Sons Ltd., 1st edn., https://doi.org/10.1002/9781118971437.ch4, 2017.

Furbish, D. J., Roering, J. J., Doane, T. H., Roth, D. L., Williams, S. G., and Abbott, A. M.: Rarefied particle motions on hillslopes - Part 1: Theory, Earth Surface Dynamics, 9, 539–576, https://doi.org/10.5194/esurf-9-539-2021, 2021.

Gardiner, C. W.: Handbook of Stochastic Methods for Physics, Chemistry and the Natural Sciences, Springer-Verlag, Berlin, https://doi.org/10.1109/jqe.1986.1073148, 1983.

Gitterman, M.: The noisy oscillator: The first 100 years, from Einstein until now, 2005.

Goh, K. I. and Barabási, A. L.: Burstiness and memory in complex systems, Europhysics Letters, 81, https://doi.org/10.1209/0295-5075/81/48002, 2008.

Guala, M., Singh, A., Badheartbull, N., and Foufoula-Georgiou, E.: Spectral description of migrating bed forms and sediment transport, Journal of Geophysical Research: Earth Surface, 119, 123–137, https://doi.org/10.1002/2013JF002759.Abstract, 2014.

Hamamori, A.: A theoretical investigation on the fluctuations of bed load transport. Technical Report No. R4., Tech. rep., Delft Hydraulics Laboratory, 1962.

Hänggi, P.: The functional derivative and its use in the description of noisy dynamical systems, in: Stochastic processes applied to physics, edited by Pesquera, L. and Rodriguez, M. A., p. 69, World Scientific Publishing Company, Santander, Spain, 1985.

Hänggi, P. and Jung, P.: Colored noise in dynamical systems, in: Advances in Chemical Physics, Volume LXXXIX, edited by Prigogine, I. and Rice, S. A., pp. 239–326, John Wiley & Sons Ltd., New York, https://doi.org/10.1002/9780470141489.ch4, 2007.

Hernández-García, E. and López, C.: Clustering, advection, and patterns in a model of population dynamics with neighborhood-dependent rates, Physical Review E, 70, 11, https://doi.org/10.1103/PhysRevE.70.016216, 2004.

Heyman, J., Ma, H. B., Mettra, F., and Ancey, C.: Spatial correlations in bed load transport : Evidence, importance, and modeling, Journal of Geophysical Research: Earth Surface, 119, 1751–1767, https://doi.org/10.1002/2013JF003003.Received, 2014.

Heyman, J., Bohorquez, P., and Ancey, C.: Entrainment, motion, and deposition of coarse particles transported by water over a sloping mobile bed, Journal of Geophysical Research: Earth Surface, 121, 1931–1952, https://doi.org/10.1002/2015JF003672, 2016.

Horsthemke, W. and Lefever, R.: Noise-Induced Transitions: Theory and Applications in Physics, Chemistry and Biology, Springer-Verlag, Berlin, 1st edn., https://doi.org/10.1007/bf00047115, 1984.

Houssais, M., Ortiz, C. P., Durian, D. J., and Jerolmack, D. J.: Onset of sediment transport is a continuous transition driven by fluid shear and granular creep, Nature Communications, 6, 1–8, https://doi.org/10.1038/ncomms7527, 2015.

Iseya, F. and Ikeda, H.: Pulsations in bedload transport rates induced by longitudinal sediment sorting: A flume study using sand and gravel mixtures, Geografiska Annaler. Series A, Physical Geography, 69, 15, https://doi.org/10.2307/521363, 1987.

Ji, C., Munjiza, A., Avital, E., Xu, D., and Williams, J.: Saltation of particles in turbulent channel flow, Physical Review E, 89, 1–14, https://doi.org/10.1103/PhysRevE.89.052202, 2014.

Kalinske, A. A.: Movement of sediment as bed load in rivers, EOS Transactions, American Geophysical Union, 28, 615–620, https://doi.org/10.1029/TR028i004p00615, 1947.

Kramers, H. A.: Brownian motion in a field of force and the diffusion model of chemical reactions, Physica, 7, 284–304, https://doi.org/10.1016/S0031-8914(40)90098-2, 1940.

Kubo, R., Toda, M., and Hashitsume, N.: Statistical Physics II: Nonequilibrium Statistical Physics, Springer-Verlag, Berlin, 1st edn., 1978.

Kumaran, V.: Granular flow of rough particles in the high-Knudsen-number limit, Journal of Fluid Mechanics, 561, 43–72, https://doi.org/10.1017/S0022112006000127, 2006.

Laio, F., Ridolfi, L., and D'Odorico, P.: Noise-induced transitions in state-dependent dichotomous processes, Physical Review E - Statistical, Nonlinear, and Soft Matter Physics, 78, 1–7, https://doi.org/10.1103/PhysRevE.78.031137, 2008.

https://doi.org/10.5194/esurf-2022-4
Preprint. Discussion started: 20 January 2022

Lajeunesse, E., Malverti, L., and Charru, F.: Bed load transport in turbulent flow at the grain scale: Experiments and modeling, Journal of Geophysical Research: Earth Surface, 115, https://doi.org/10.1029/2009JF001628, 2010.

Lajeunesse, E., Devauchelle, O., and James, F.: Advection and dispersion of bed load tracers, Earth Surface Dynamics, 6, 389–399, https://doi.org/10.5194/esurf-6-389-2018, 2017.

Laskin, N.: Non-Gaussian diffusion, Journal of Physics A: Mathematical and General, 22, 1565–1576, 1989.

Lee, D. B. and Jerolmack, D.: Determining the scales of collective entrainment in collision-driven bed load, Earth Surface Dynamics, 6, 1089–1099, https://doi.org/10.5194/esurf-6-1089-2018, 2018.

Lisle, I. G., Rose, C. W., Hogarth, W. L., Hairsine, P. B., Sander, G. C., and Parlange, J. Y.: Stochastic sediment transport in soil erosion, Journal of Hydrology, 204, 217–230, https://doi.org/10.1016/S0022-1694(97)00123-6, 1998.

Lisle, T. E., Iseya, F., and Ikeda, H.: Response of a channel with alternate bars to a decrease in supply of mixed-size bed load: A flume experiment, Water Resources Research, 29, 3623–3629, https://doi.org/10.1029/93WR01673, 1993.

Liu, M. X., Pelosi, A., and Guala, M.: A statistical description of particle motion and rest regimes in open-channel flows under low bedload transport, Journal of Geophysical Research: Earth Surface, 124, 2666–2688, https://doi.org/10.1029/2019JF005140, 2019.

Łuczka, J.: Non-Markovian stochastic processes: Colored noise, Chaos, 15, https://doi.org/10.1063/1.1860471, 2005.

Łuczka, J., Niemiec, M., and Piotrowski, E.: Linear systems with randomly interrupted Gaussian white noise, Journal of Physics A: Mathematical and General, 26, 4849–4861, https://doi.org/10.1088/0305-4470/26/19/018, 1993.

Madej, M. A., Sutherland, D. G., Lisle, T. E., and Pryor, B.: Channel responses to varying sediment input: A flume experiment modeled after Redwood Creek, California, Geomorphology, 103, 507–519, https://doi.org/10.1016/j.geomorph.2008.07.017, 2009.

Mao, L.: The effect of hydrographs on bed load transport and bed sediment spatial arrangement, Journal of Geophysical Research: Earth Surface, 117, 1–16, https://doi.org/10.1029/2012JF002428, 2012.

Martin, R. L., Jerolmack, D. J., and Schumer, R.: The physical basis for anomalous diffusion in bed load transport, Journal of Geophysical Research: Earth Surface, 117, 1–18, https://doi.org/10.1029/2011JF002075, 2012.

Masoliver, J.: Second-order dichotomous processes: Damped free motion, critical behavior, and anomalous superdiffusion, Physical Review E, 48, 121–135, https://doi.org/10.1103/PhysRevE.48.121, 1993.

McDowell, C. and Hassan, M. A.: The influence of channel morphology on bedload path lengths: Insights from a survival process model, Earth Surface Processes and Landforms, 45, 2982–2997, https://doi.org/10.1002/esp.4946, 2020.

Menzel, A. M. and Goldenfeld, N.: Effect of Coulombic friction on spatial displacement statistics, Physical Review E, 84, 1–9, https://doi.org/10.1103/PhysRevE.84.011122, 2011.

Michaelides, E. E.: Review — The transient equation of motion for particles, bubbles, and droplets, Journal of Fluids Engineering, Transactions of the ASME, 119, 233–247, https://doi.org/10.1115/1.2819127, 1997.

Nakagawa, H. and Tsujimoto, T.: On probabilistic characteristics of motion of individual sediment particles on stream beds, in: Hydraulic Problems Solved by Stochastic Methods: Second International IAHR Symposium on Stochastic Hydraulics, pp. 293–320, Water Resources Publications, Lund, Sweden, 1976.

Olivares-Robles, M. A. and García-Colin, L. S.: On different derivations of telegrapher's type kinetic equations, Journal of Non-Equilibrium Thermodynamics, 21, 361–379, https://doi.org/10.1515/jnet.1996.21.4.361, 1996.

Papanicolaou, A. N., Tsakiris, A. G., Wyssmann, M. A., and Kramer, C. M.: Boulder array effects on bedload pulses and depositional patches, Journal of Geophysical Research: Earth Surface, 123, 2925–2953, https://doi.org/10.1029/2018JF004753, 2018.

https://doi.org/10.5194/esurf-2022-4
Preprint. Discussion started: 20 January 2022

Parker, G., Paola, C., and Leclair, S.: Probabilistic Exner sediment continuity equation for mixtures with no active layer, Journal of Hydraulic Engineering, 128, 801, https://doi.org/10.1061/(ASCE)0733-9429(2002)128:8(801), 2000.

Pechenik, L. and Levine, H.: Interfacial velocity corrections due to multiplicative noise, Physical Review E, 59, 3893–3900, https://doi.org/10.1103/PhysRevE.59.3893, 1999.

Pierce, J. K.: The stochastic movements of individual streambed grains, Ph.D. thesis, The University of British Columbia, 2021.

Prudnikov, A. P., Brychkov, I. A., Marichev, O. I., and Gould, G. G.: Integrals and Series Vol. 5: Inverse Laplace Transforms, Gordon and Breach Science Publishers, Paris, 1992.

Recking, A., Liébault, F., Peteuil, C., and Jolimet, T.: Testing bedload transport equations with consideration of time scales, Earth Surface Processes and Landforms, 37, 774–789, https://doi.org/10.1002/esp.3213, 2012.

Risken, H.: The Fokker-Planck Equation: Methods of Solution and Applications, Springer-Verlag, Ulm, 2nd edn., https://doi.org/10.1080/713821438, 1984.

Roseberry, J. C., Schmeeckle, M. W., and Furbish, D. J.: A probabilistic description of the bed load sediment flux: 2. Particle activity and motions, Journal of Geophysical Research: Earth Surface, 117, https://doi.org/10.1029/2012JF002353, 2012.

Saletti, M., Molnar, P., Zimmermann, A., Hassan, M. A. ., and Church, M.: Temporal variability and memory in sediment transport in an experimental step-pool channel, Water Resources Research, 51, 9325–3337, https://doi.org/10.1111/j.1752-1688.1969.tb04897.x, 2015.

Schmeeckle, M. W.: Numerical simulation of turbulence and sediment transport of medium sand, Journal of Geophysical Research: Earth Surface, 119, 1240–1262, https://doi.org/10.1002/2013JF002911, 2014.

Schmeeckle, M. W. and Nelson, J. M.: Direct numerical simulation of bedload transport using a local, dynamic boundary condition, Sedimentology, 50, 279–301, https://doi.org/10.1046/j.1365-3091.2003.00555.x, 2003.

Schmeeckle, M. W., Nelson, J. M., and Shreve, R. L.: Forces on stationary particles in near-bed turbulent flows, Journal of Geophysical Research: Earth Surface, 112, 1–21, https://doi.org/10.1029/2006JF000536, 2007.

Singh, A., Fienberg, K., Jerolmack, D. J., Marr, J., and Foufoula-Georgiou, E.: Experimental evidence for statistical scaling and intermittency in sediment transport rates, Journal of Geophysical Research: Earth Surface, 114, 1–16, https://doi.org/10.1029/2007JF000963, 2009.

Strom, K., Papanicolaou, A. N., Evangelopoulos, N., and Odeh, M.: Microforms in gravel-bed rivers: formation, disintegration, and effects on bedload transport, Journal of Hydraulic Engineering, 130, 554–567, https://doi.org/10.1061/(ASCE)0733-9429(2004)130, 2004.

Taylor, G. I.: Diffusion by continuous movements, Proceedings of the London Mathematical Society, s2-20, 196–212, https://doi.org/10.1063/1.1691776, 1920.

Turowski, J. M.: Probability distributions of bed load transport rates: A new derivation and comparison with field data, Water Resources Research, 46, https://doi.org/10.1029/2009WR008488, 2010.

Van Kampen, N. G.: Stochastic Processes in Physics and Chemistry, Elsevier B.V., 3rd edn., https://doi.org/10.1016/B0-12-369401-9/00623-9, 2007.

Wang, M. C. and Uhlenbeck, G.: On the theory of Brownian motion II, Reviews of Modern Physics, 17, 323–342, https://doi.org/10.1007/BF01020584, 1945.

Weiss, G. H.: Aspects and Applications of the Random Walk., North Holland, Amsterdam, https://doi.org/10.2307/2291190, 1994.

Weiss, G. H.: Some applications of persistent random walks and the telegrapher's equation, Physica A: Statistical Mechanics and its Applications, 311, 381–410, https://doi.org/10.1016/S0378-4371(02)00805-1, 2002.

Williams, S. and Furbish, D.: Particle energy partitioning and transverse diffusion during rarefied travel on an experimental hillslope, Earth Surface Dynamics Discussions, pp. 1–33, https://doi.org/10.31223/X58K5N, 2021.

https://doi.org/10.5194/esurf-2022-4
Preprint. Discussion started: 20 January 2022

Wong, M. and Parker, G.: Reanalysis and correction of bed-load relation of Meyer-Peter and Müller using their own database, Journal of Hydraulic Engineering, 132, 1159–1168, https://doi.org/10.1061/(ASCE)0733-9429(2006)132:11(1159), 2006.